Highly Efficient InGaN-Based Light Emitting Devices grown on Nanoscale Patterned Substrates by MOCVD

Chien-Chung Lin[a,*], Ching-Hsueh Chiu[b], H.W. Huang[b], Shih-Pang Chang[b], Hao-Chung Kuo[b,*], and Chun-Yen Chang[c]

[a]Institute of Photonic System, College of Photonics, National Chiao-Tung University, Tainan, Taiwan
[b]Department of Photonics, National Chiao-Tung University, Hsinchu, Taiwan
[c]Department of Electronics Engineering, National Chiao Tung University, 1001 Ta Hsueh Rd., Hsinchu, Taiwan
e-mail: chienchunglin@faculty.nctu.edu.tw; hckuo@faculty.nctu.edu.tw

ABSTRACT

Highly efficient InGaN-base light emitting diodes are crucial for next generation solid state lighting. However, drawbacks in substrate materials such as lattice and thermal expansion coefficient mismatches hold back the lamination efficiency improvement. In the past, patterned sapphire sustrate (PSS) has been proven to be effect to enhance the LED's performance. In this work, we reviewed several promising nano-scale technologies which successfully increase the output of LED through better material quality and light extraction. First, we presented a study of high-performance blue emission GaN LEDs using GaN nanopillars (NPs). It exhibits smaller blue shift in electroluminescent peak wavelength and great enhancement of the light output (70% at 20 mA) compared with the conventional LEDs. Secondly, GaN based LEDs with nano-hole patterned sapphire (NHPSS) by nano-imprint lithography are fabricated structure grown on sapphire substrate. At an injection current of 20mA, the LED with NHPSS increased the light output power of LEDs by 1.33 times, and the wall-plug efficiency is 30% higher at 20mA indicating that it had larger light extraction efficiency (LEE). Finally, we fabricated the high performance electrical pumping GaN-based semipolar {10-11} nano-pyramid LEDs on c-plane sapphire substrate by selective area epitaxy (SAE). The emission wavelength only blue-shifted about 5nm as we increased the forward current from 40 to 200mA, and the quantum confine stark effect (QCSE) had been remarkably suppressed on semipolar surface at long emission wavelength region. These results manifest the promising role of novel nanotechnology in the future III-nitride light emitters.

Keywords: light emitting devises (LEDs), light extraction efficiency (LEE), selective area epitaxy (SAE), quantum confine stark effect (QCSE)

1. INTRODUCTION

GaN-based optoelectronic devices can be used in a wide range of applications due to its wide band gap coverage (from ultraviolet to infrared), sustainability of high electrical field and high temperature operation. In last two decades, we saw a strong, and growing demand of GaN-based lasers or light emitting diodes (LEDs) which will eventually change our daily life. However, lack of a suitable, inexpensive substrate restrains the improvement of GaN-based devices. Even though many semiconductor companies produce and sell pure GaN substrates today, their prices are high and not very accessible to ordinary applications. Typically, GaN-based epitaxial layers were grown on sapphire substrate by heteroepitaxial technique, such as metal-organic chemical vapor deposition (MOCVD) [1]. Due to the large lattice mismatch and thermal expansion coefficient misfit between GaN and sapphire, the subsequent-grown GaN epitaxial

Display, Solid-State Lighting, Photovoltaics, and Optoelectronics in Energy III, edited by Min Gu, Franky So, Xiao Wei Sun,
Proc. of SPIE-OSA-IEEE Asia Communications and Photonics, SPIE Vol. 8312, 83120C · © 2011 SPIE-OSA-IEEE
CCC code: 0277-786X/11/$18 · doi: 10.1117/12.915513

layers usually contained high threading dislocation densities (TDDs) (around 10^8-10^{10} cm^{-2}) [2]. To improve the crystalline quality of GaN-based epitaxial layers on sapphire substrate, various growth techniques have been proposed, such as epitaxial lateral overgrowth (ELO) [3], cantilever epitaxy (CE) [4], defect selective passivation [5], microscale SiN_x or SiO_x patterned mask [6], anisotropically etched GaN-sapphire interface [7], plastic relaxation through buried AlGaN cracks [8], and patterned sapphire substrate (PSS) [9]. Meanwhile, theoretical and experimental studies indicate that a further reduction in defect density is possible if the lateral overgrowth approach is extended to the nanoscale [10]. In this study, we will review and demonstrate several promising nanotechnologies for highly efficient InGaN-based light emitting devices.

2. NANO-TECHNOLOGIES FOR ENHANCEMENT OF LED PERFORMANCE

As we point out in the previous section, there are several available technologies for LED industry to adapt these days, and they can be very effective in terms of increasing light output. The common features for these different fabrication techniques are the reduction of dislocation density through the epitaxy and the increased light extraction efficiency (LEE). The former factor is a direct result of nano-scale patterning and usually rises from the epitaxial lateral overgrowth (ELOG) phenomenon occurred often in GaN related materials. The latter factor is due to the extra light scattering coming from the discontinuity of the GaN material and the introduction of air-void or other nano-size structures. In the following, we will review several promising methods which can improve the output power of the regular LED design. All these methods are based on our understanding of nano-fabrication technologies.

2.1 Highly Efficient and Bright LEDs Overgrown on GaN Nano-Pillar Substrates

The epitaxial structure for GaN-based LED on sapphire with GaN nano-pillars (NPs) was prepared as follows. First, the self-assembled GaN NP structure was grown on sapphire substrate by a RF-plasma MBE system (ULVAC MBE), and the related processes have been reported in our previous study. Fig. 1 (a) shows scanning electron microscope (SEM) image of the grown GaN NPs. It can clearly be seen that the GaN NP is in funnel-like form shown on the inset Fig. 1 (a), which might be beneficial for the following re-growth of GaN-based LED structure. In addition, the density, diameter and the height of the nano-pillars are estimated to be around $1.15\times10^{10}\,cm^{-2}$, 50 nm and 0.8 μm, respectively. Next, we deposited a GaN-based LED structure on this nano-pillar template by a low pressure MOCVD (Veeco D75) system, denoted as NP-LEDs as shown in Fig. 1 (b). In the mean time, the same GaN-based LED structure was also grown on sapphire without GaN NP for comparison, denoted as conventional LEDs (i.e., C-LEDs).

After the u-GaN layer was deposited, without growth of remaining LED layers, the surface morphology was measured by AFM, as shown in Fig. 2. The root mean square (RMS) value of the surface roughness is about 1.4 nm, indicating high surface quality and excellent coalescence overgrown on GaN NPs template. To analyze the detailed epitaxial layer quality, we used TEM to compare the cross section between two types of devices (NP-LEDs and C-LEDs). As we can see from Fig. 3 (a), in the case of the GaN epitaxial layer grown on sapphire without GaN NPs,

numbers of threading dislocation propagate vertically from the interface of GaN and sapphire, all the way to the top device layers. As a result, the TDs density in conventional GaN layer can be as high as 10^9 cm^{-2}. Whereas, for the GaN epitaxial layer grown on sapphire with GaN NP (Fig. 3 (b)), it can be clearly found that the crystallography is drastically different from that of conventional ones. Fewer TDs are observable within the range in view. The dislocation density on the top of *n*-GaN, MQWs is calculated to be around 7×10^7 cm^{-2}. The reduction of TDs density can be attributed to the misfit (mainly perpendicular to the c-axis) and dislocation bending occurred just above the voids, as shown in the inset of Fig. 3 (b). Such behaviors are similar to those occurred in the nanoscale epitaxial lateral overgrowth (NELOG) method on a SiO_2 nanorod-array patterned sapphire substrate.

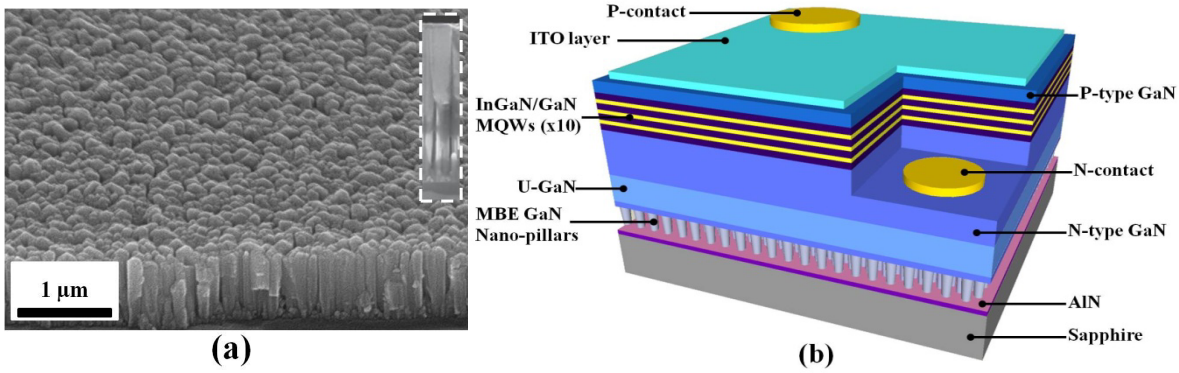

Fig. 1. (a) Cross-sectional SEM image of GaN NPs template. The inset shows the funnel-like GaN NP. (b) Schematic of GaN-based LED structures on GaN NPs template.

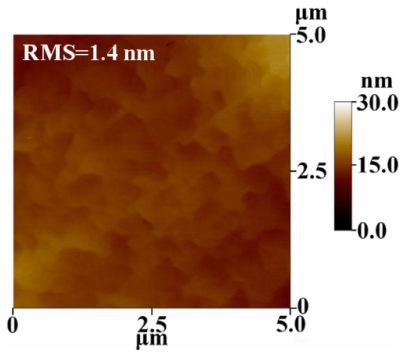

Fig. 2. Surface morphology of overgrown GaN NPs template scanned by AFM.

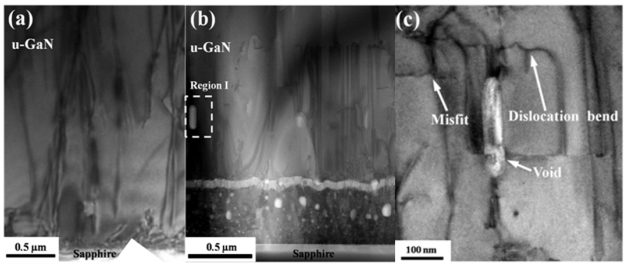

Fig. 3. TEM image of (a) C-LEDs, (b) NP-LEDs, (c) High resolution TEM image of region I in (b). The diffraction condition is *g*=0002.

Fig. 4 (a) shows EL emission peak wavelength as a function of injection current for NP-LEDs and C-LEDs. The emission peak wavelength of NP-LED is slightly red-shifted (about 3.4 nm) from that of C-LED, and this is reasonable since lateral strain relaxation favors higher indium incorporation. More importantly, as we increase the injection current, the emission peak wavelength of NP-LEDs exhibits smaller blueshift (around 2.9 nm) compared with that of C-LEDs

(around 5.6 nm). This result indicates that the QCSE does become weaker due to the strain relaxation in epitaxial layer overgrown on GaN NPs template, as we expected. Fig. 4 (b) displays the typical power-current-voltage (L-I-V) characteristics of NP-LEDs and C-LEDs. With an injection current of 20 mA, the forward voltages are 3.38 and 3.40 V, and the output powers are 25.3 and 14.8 mW, for NP-LEDs and C-LEDs, respectively. The light enhancement of L-I-V characteristics can be attributed to the following factors: First, the TD density reduction of epitaxial layers. This reduction leads to much fewer non-radiative recombination events in the nano-pillar devices and increases the photon generation efficiency. Second, more lights can be extracted from the LED because of the light scattering effect from the embedded nano-scale air voids.

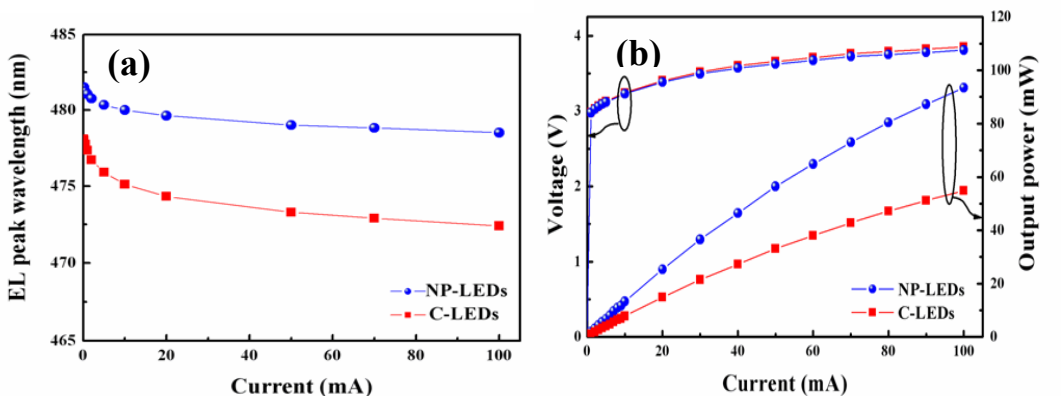

Fig. 4. (a) The EL peak wavelength as a function of injection current of two fabricated LEDs. (b) L-I-V characteristics of the two fabricated LEDs.

2.2 Investigation of GaN-based light emitting diodes with nano-hole patterned sapphire substrate (NHPSS) by nano-imprint lithography

Fig. 5 shows the schematic structure of LED with NHPSS. In our study, this type of sample is fabricated in order to understand the influence of the NHPSS on the LED output power performance. LED structure consists of a Cr/Pt/Au p-electrode, ITO transparent layer, LED epitaxial layers, a smooth p-GaN surface, and a Cr/Pt/Au n-electrode on NHPSS. Fig. 6(a) top-view and (b) cross-section of SEM images of sapphire with NHPSS. Fig. 6(a) SEM image shows the nano-hole dimension and pattern pitch were approximately 240 and 450 nm. Fig. 6(b) SEM image shows the 12-fold photonic quasi-crystal pattern based on square-triangular lattice (in Fig. 6(b) left-side model). We choose the 12-fold photonic quasi-crystal pattern due to the better enhancement of surface emission was obtained from the PCs with a dodecagonal symmetric quasi-crystal lattice than regular PCs with triangular lattice and 8-fold PQC [11]. The recursive tiling of offspring dodecagons packed with random ensembles of squares and triangles in dilated parent cells forms the lattice. Additionally, in this case we using the dry etching depth and sidewall angle of NHPSS were approximately 165nm and 45◦. We design the 450nm pattern pitch of PQC in this experiment; the 450nm pitch is the optimum for the light emission on 460nm of wavelength.

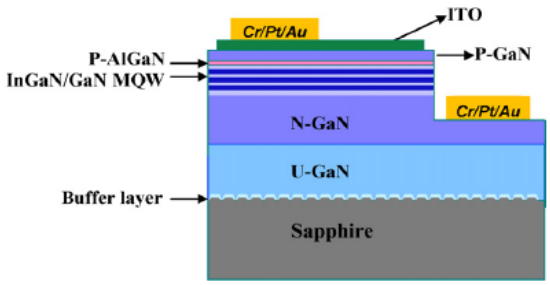

Fig. 5. Schematic diagram of LEDs structure with NHPSS

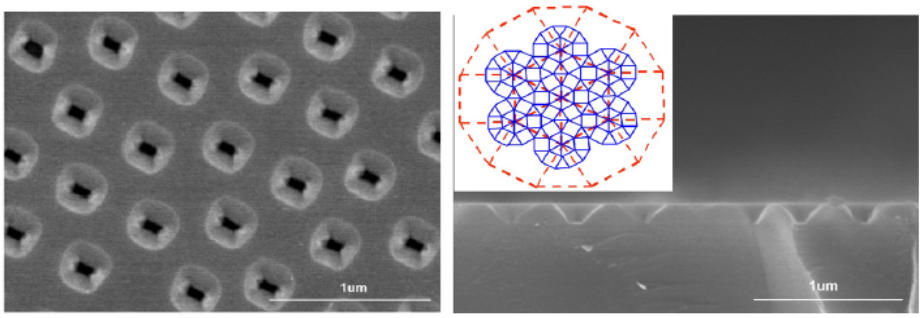

Fig. 6. (a) Top-view and (b) cross-section (inset 12-fold photonic quasi-crystal model) SEM images of sapphire surface with NHPSS.

The light output is detected by calibrating an integrating sphere with Si photodiode on the package device, so that light emitted in all directions from the LED can be collected. The intensity–current (*L–I*) characteristics of the LEDs with and without NHPSS are shown in Fig. 7. At an injection current of 20mA and peak wavelength of 455nm for TO (Transistor Outline)-can package, the light output powers of LED without NHPSS, and LED with NHPSS (etching depth = 165 nm) on TO-can are given by 14.0 and 18.7mW, respectively. Hence, the enhancement percentages of LED with NHPSS (etching depth = 165 nm) is 33%, respectively, compared to that of LED without NHPSS. The higher enhancement on standard LED type addresses the effect of the NHPSS which maybe allows the reflect light from sapphire substrate onto the top direction and higher epitaxial crystal quality to increase more light output power. If GaN-based LED on sapphire substrate with metallization reflector compared with NHPSS. The simple backside metallization only can increase the EL intensity, but it cannot increase the light output power unless backside reflector of LED with omnidirectional reflector. In addition, the corresponding wall-plug efficiencies (WPE) of conventional LED, LED with NHPSS were 23%, and 30%, respectively, which addresses a substantially improvement by the NHPSS structures as well at a driving current of 20mA.

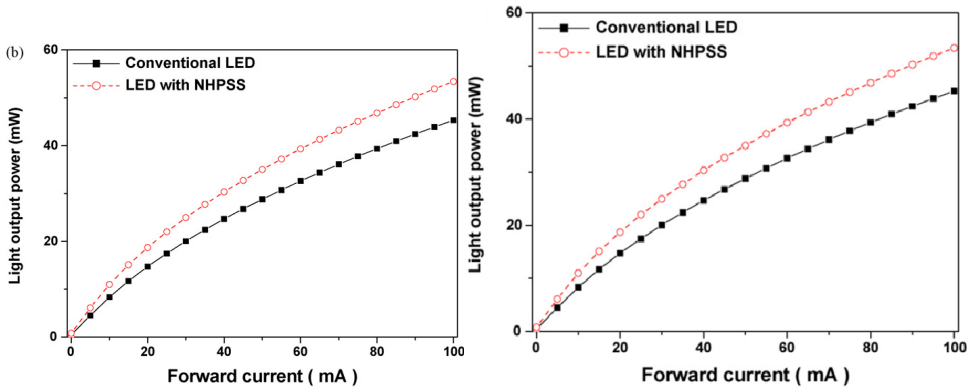

Fig. 7. Light output power–current (*L–I*) characteristics of LED with/without NHPSS, respectively.

2.3 Fabrication of green emission Semipolar {1011} InGaN/GaN Nanopyramid LEDs

In order to grow semipolar {10-11} facets of GaN nanopyramid arrays, a 2 μm thick GaN film grown on sapphire was processed into GaN nanorods firstly by nano-imprint-lithography (NIL). Next, the well aligned cylindrical shape GaN nanorods have been fabricated after NIL dry etching process. The diameter and the periodicity of GaN nanorods are 350 nm and 750 nm, respectively. Then, the side wall of GaN nanorods were passivated with 30 nm thick dielectric material by spin on glass (SOG) technique and the dry etching process was applied to make sure the appearance of the top of GaN nanorods. The GaN nanopyramids and 10 pairs $In_{0.3}Ga_{0.7}N$ (3 nm)/GaN (8nm) MQWs were selectively grown on the top of the GaN nanorods in sequence by AXITRON 2000HT metalorganic chemical vapor deposition (MOCVD) reactor. While the InGaN well and GaN barrier were grown at the same growth pressure of 300 mbar, but at different temperatures of 710℃ and 795℃, respectively. The 20nm p-type AlGaN was adopted as the electron blocking layer and a 200nm p-type GaN was applied as the p-type layer. Finally, the complete epitaxial structure processed by standard LED fabrication flow into a chip size 300×300 μm^2, and the lateral schematic structure of was shown in the Fig. 8.

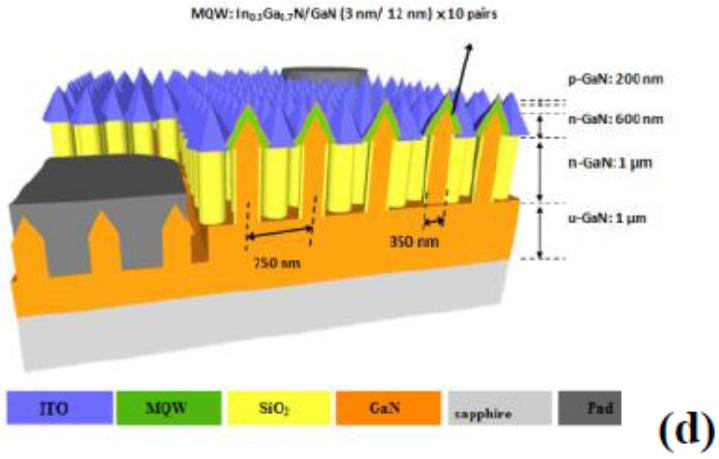

Fig.8. lateral schematic illustration of nanopyramid LED

Fig. 9 (a) shows the output power density and forward voltage versus injection current (L-I-V) of green emission nanopyramid LEDs, and the operation image under forward current 50 mA is inserted in the background. Since the total active area of nanopyramid LED is estimated to be two times larger than planar c-plane LED, for comparing these two types of LED under the same equivalent current density. The injected current of nanopyramid LEDs must be doubled than planar LEDs. The light output power density of green nanopyramid LEDs is as high as 1500 mW/cm^2 at 40 mA and the corresponding forward voltage (V_f) and series resistance (R_s) are 3.61 V and 2.5 Ω respectively. The electrical properties are comparable with conventional cplane LEDs [12].

Fig. 9 (b) shows the current-dependent electroluminescence (EL) spectrum of green nanopyramid LEDs. There are two main peaks in the EL spectra, the emission peaks change with the same tendency as increasing the forward current. The significant blue shift under low injection current was attributed by carriers filling in localized state. The peak wavelength only made a 5nm blue shift from 40 mA to 200mA and stabilized at 495nm, which evinced the low IEF properties of semipolar MQWs.

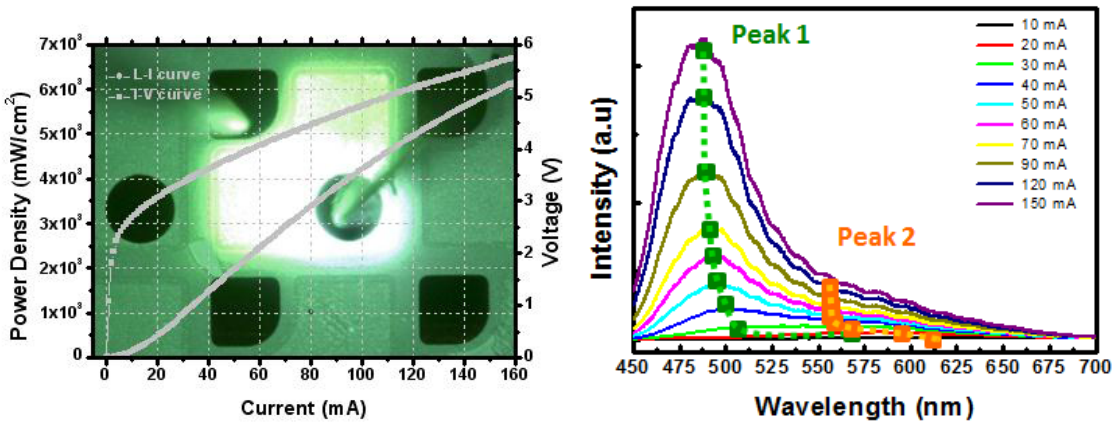

Fig. 9. (Color online) (a) The L-I-V curve; (b) The EL emission spectrum of green nanopyramid LEDs.

3. CONCLUSION

In conclusion, we reviewed the latest advancements of the nano fabrication technologies for LED and their impacts towards the performances of devices. While there are several applicable methods at present, more developments are possible with the progress in the nanofabrication. We will embrace these changes and work towards a more commercially-viable, technology superior design for the future solid state lighting.

4. REFERENCE

1. E. F. Schubert, *Light Emitting Diodes*, (Cambridge University Press, Cambridge, 2003), 2nd ed, pp 21-22.
2. S. Nakamura, M. Senoh, S. Nagahama, N. Iwasa, T. Yamada, T. Matsushita, H. Kiyoku, Y. Sugimoto, T. Kozaki, H. Umemoto, M. Sano, and K. Chocho, *Appl. Phys. Lett.,* vol. 72, pp. 211, 1998.
3. Tsvetanks S. Zheleva, Ok-Hyun Nam, Michael D. Bremser, and Robert F. Davis, *Appl. Phys. Lett.,* vol.71, pp. 2472, 1997.
4. D. M. Follstaedt, P. P. Provencio, N. A. Missert, C. C. Mitchell, D. D. Koleske, A. A. Allerma, and C. I. H. Ashby, *Appl. Phys. Lett.,* vol. 81, pp. 2758, 2002.
5. M. H. Lo, P.M. Tu, C.H. Wang, Y.J. Cheng, C.W. Hung, S.C. Hsu, H.C. Kuo, H.W. Zan, S. C. Wang, C.Y. Chang, and C.M. Liu, *Appl. Phys. Lett.,* vol. 95, pp. 211103, 2009.

6. A. Sakai, H. Sunakawa, and A. Usui, *Appl. Phys. Lett.,* vol. 71, pp. 2259, 1997.
7. M. H. Lo, P. M. Tu, C. H. Wang, C. W. Hung, S. C. Hsu, Y. J. Cheng, H. C. Kuo, H. W. Zan, S. C. Wang, C. Y. Chang, and S. C. Huang, *Appl. Phys. Lett.,* vol. 95, pp. 041109, 2009.
8. J.-M. Bethoux, P. Vennéguès, F. Natali, E. Feltin, O. Tottereau, G. Nataf, P. De Mierry, and F. Semond , *J. Appl. Phys.,* vol. 94, pp. 6499, 2003.
9. Y. J. Lee, J. M. Hwang, T. C. Hsu, M. H. Hsieh, M. J. Jou, B. J. Lee, T.C. Lu, H.C. Kuo, and S.C. Wang, *IEEE Photon. Technol. Lett.* vol. 18, pp. 1152, 2006.
10. Yik-Khoon Ee, Jeffrey M. Biser, Wanjun Cao, Helen M. Chan, Richard P. Vinci, and Nelson Tansu, IEEE J. Sel. Top. Quantum Electron., vol. 15, pp. 1066-1072, 2009.
11. Z. S. Zhang, B. Zhang, J. Xu, K. Xu, Z.J. Yang, Z.X. Qin, T.J. Yu, D.P. Yu, Appl. Phys. Lett. 88 (2006) 171103.
12. C. Y. Cho, S. H. Han, S. J. Lee, S. C. Park, and S. J. Parkz, "Green Light-Emitting Diodes on Semipolar {11(2)over-bar2} Microfacets Grown by Selective Area Epitaxy, "JES, 157 (1)H86-H89 (2010).